Journal of ELECTRONIC MATERIALS, Vol. 48, No. 4, 2019
https://doi.org/10.1007/s11664-019-06997-y

Sliding Mode Control for MPPT of a Thermogenerator

SEDDIK BENHADOUGA,[1,2] MOUNIR MEDDAD,[1,2] ADIL EDDIAI ,[3,5] DJAMEL BOUKHETALA,[4] and RIAD KHENFER[1,2]

1.—Université Mohamed El Bachir El Ibrahimi de Bordj Bou Arreridj, Bordj Bou Arreridj, Algeria. 2.—Laboratoire d'Automatique de Sétif (LAS), Université Ferhat Abass de Setif, Sétif, Algeria. 3.—Laboratoire de Physique de la Matière Condensée, Faculté des Sciences Ben M'sik, Université Hassan II de Casablanca, Casablanca, Morocco. 4.—Laboratoire de Commande des Processus (LCP), ENP, El Harrach, Algeria. 5.—e-mail: aeddiai@gmail.com

This paper reports a practical implementation for maximum power point tracking (MPPT) of a thermoelectric generator (TEG) module using sliding mode control. The principal goal is to apply a robust technique of control to ensure maximum power transfer towards the load through a boost converter. On the one hand, the proposed technique improves rapidly the effect of load variation, and on the other hand, it increases the overall performance of the system. The MPPT control is modeled in Simulink/Matlab with the theoretical Models of a TEG module and a boost converter. Simulation results give the sliding mode control performance under different temperature gradients. Hardware based on an Arduino card is implemented, where the experimental results are presented and analyzed. The experimental results are compared with simulation data where a good agreement is observed. Finally, the results show the effectiveness and the robustness of sliding mode control.

Key words: Thermogenerator, MPPT control, sliding mode control, prototype

INTRODUCTION

In recent years, energy production has been a great challenge of industrialized societies for their energy needs. Also, applications of embedded systems and micro-systems will need more energy autonomy to carry out good functioning. Today, a large part of global energy production comes from fossil sources which cause pollution and stockpile reduction of this type of energy, that have led to the use of these devices.[1–3]

Renewable energies are unlimited energy resources, which come from the sun, wind, heat of the earth, water or biomass, including a number of technological fields valued according to energy source and useful energy quantity obtained.[4–7] Among these approaches, heat energy harvesting via thermoelectric generators (TEGs) converts thermal energy into electrical energy without any mechanical moving parts.

(Received April 12, 2018; accepted January 23, 2019; published online February 8, 2019)

The TEGs are solid modules, comprising a group of thermocouple elements interconnected and used in the harvesting power supplies sources of many intelligent applications. Thermoelectric energy comes from the direct conversion of thermal energy into electrical parts, or electric energy can be converted into thermal energy for cooling or heating demands.[8–11]

The efficiency of the TEG majorly depends on the temperature gradient applied between the two junctions. In order to extract the maximum power at the terminals of the TEG, an adaptation stage between the generator and the load is introduced to couple the two elements as perfectly as possible. But, the problem of transferring the maximum power of TEG to the load is a key point of this study.

Many studies are focused on optimal electrical load matching conditions for maximizing power generation and applying maximum power point tracking (MPPT) standard algorithms, such as perturb, observe (P&O), incremental conductance (IC), Lock-On Mechanism, .0Measuring a fraction of the open-circuit voltage (FCO) and proportional integral (PI).[1–13]

This paper is to present a validation of novel technical control, sliding mode control (SMC) applied to the TEG for MPPT, which is based on controlling a power boost converter which operates under many operating points. These MPPT controls have originally been applied for PV systems.[10–13]

This paper is organized as follows: the modeling and simulation of operational characteristics of TEG devices are described in the "Thermoelectric Generator Modeling" section; the proposed sliding mode control for the MPPT system is presented briefly in the "Simulation Results" section and the different equipment (hardware and software) used in this paper are introduced in the "Experimental Data Acquisition" section.The last section is devoted to the implementation and presentation of experimental results of the proposed control. Finally, this work will close with a general conclusion through which are presented the main results.

THERMOELECTRIC GENERATOR MODELING

Thermoelectricity

The thermoelectricity is a phenomenon that allows the conversion of thermal energy into electrical energy through a temperature gradient. This phenomenon was discovered in 1821 and is called the "Seebeck effect," while the reverse counterpart of this phenomenon was discovered by Peltier in 1834.[10,14] Figure 1 illustrates the operating principle of this phenomenon.

Many advantages of this energy-conversion phenomenon include solid-state operation, having no moving parts; they do not cause any vibrations in the application, vast scalability, maintenance-free operation vis-à-vis the lack of moving parts or chemical reactions, and a long duration span of reliable operation.[15–18] Thermoelectric generators (TEGs) generate electric direct current (DC) in a closed-circuit through a load when a temperature gradient develops between the two ends of the device, therefore, no rectification is needed.[19,20] The coupling effects managing the conversion are the Seebeck, Peltier, Thomson, and Joule effects. Understanding the transient behavior of TEG is very important so as to optimize the energy harvesting from waste heat, when one junction is exposed to an unsteady heat source and the other is subjected to natural convection at ambient temperature. Several models have been developed for each configuration,[21–23] but most models assume either an unlimited heat source or steady-state methods of operation. Practical applications such as being parasitic of energy harvested starting at waste heat sources generally have unsteady heat flux and/or temperature conditions on the hot side of the TEG that pose a fully coupled thermoelectric problem.[24]

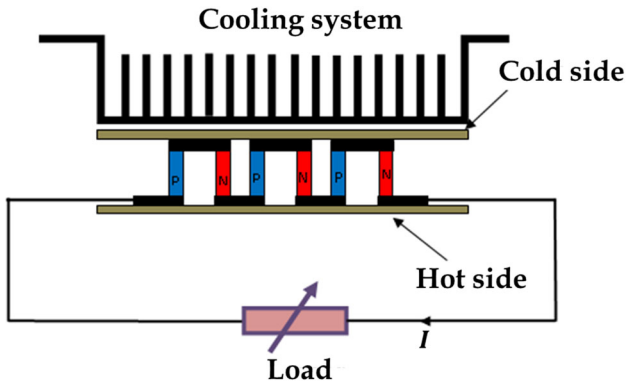

Fig. 1. Schematic diagram of a typical TEG. Reprinted with permission of Ref. 14.

Electrical Model of TEG

In literature, TEGs are mostly considered under invariable temperature gradient conditions.[25,26] The influence of the internal contact thermal resistance is generally neglected. Under these conditions, the equivalent electrical circuit of TEG can analytically be modeled with a constant voltage source in series with an internal resistance R_{TEG}. According to Seebeck's effect, the open-circuit voltage V_{oc}, of the TEG is enclosed in the thermal energy, which is composed of η thermocouples connected electrically in series and thermally in parallel.[14,27]

Where given by

$$V_{\mathrm{oc}} = S.\Delta T = \eta.\alpha(T_h - T_c). \tag{1}$$

where S represent the Seebeck coefficient of a TEG module (α is the Seebeck coefficient of a thermocouple between the p and n semiconductors) and η is the number of thermocouples.

T_h, T_c are the temperatures of the hot-side and the cold-side, respectively.

The harvested current I_{TEG}, when a gradient of temperature is applied ΔT, is given by the following equation:

$$I_{\mathrm{TEG}} = \frac{V_{\mathrm{oc}} - V_{\mathrm{TEG}}}{R_{\mathrm{TEG}}} = \frac{\eta.\alpha(T_h - T_c) - V_{\mathrm{TEG}}}{R_{\mathrm{TEG}}}. \tag{2}$$

The output power P_{TEG} handed over to the load R_L by the TEG, can be determined by using Eq. 2 and the output voltage V_{TEG} of TEG, which is given by

$$P_{\mathrm{TEG}} = V_{\mathrm{TEG}}.I_{\mathrm{TEG}} = V_{\mathrm{TEG}}.\frac{\eta.\alpha(T_h - T_c) - V_{\mathrm{TEG}}}{R_{\mathrm{TEG}}}. \tag{3}$$

The model of TEG with simulink/Matlab is presented in Fig. 2.

The model of a TEG module with Matlab/Simulink is shown in Fig. 2, which is decomposed into two parts, the first is the voltage V_{oc} of Eq. 1

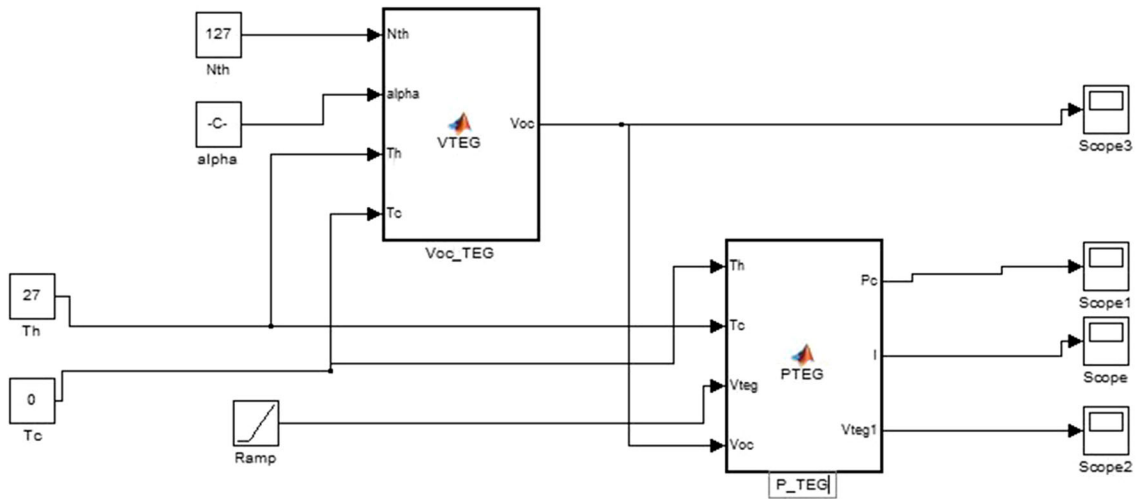

Fig. 2. Simulink/Matlab model of TEG. Reprinted with permission of Ref. 14.

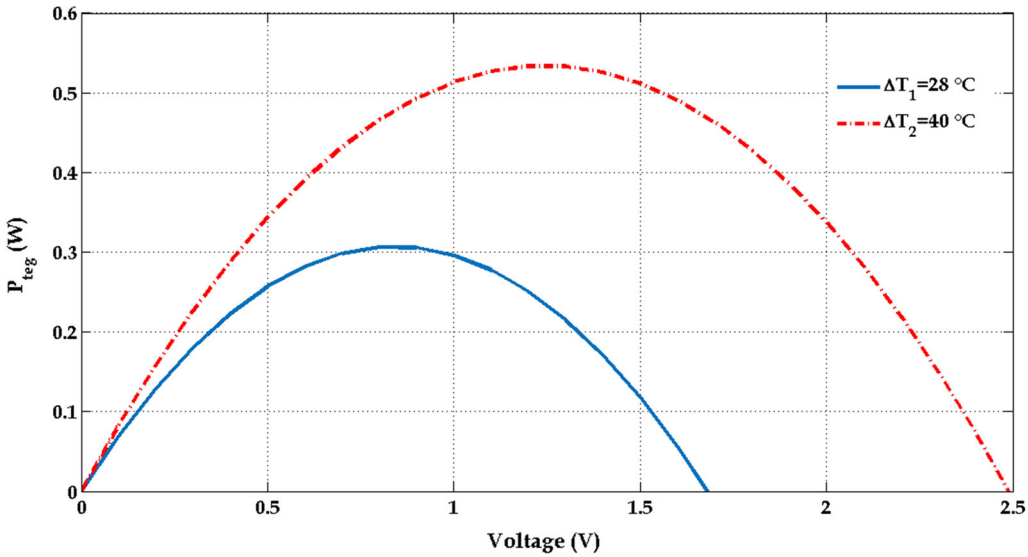

Fig. 3. *P–V* curve of TEG (TEC1-12706). Reprinted with permission of Ref. 14.

and the second represent the power generated by the TEG module given by Eq. 3.

SIMULATION RESULTS

The simulation results of the *P–V* curve and *P–R* curve of one TE module generator TEC1-12706 for different temperature gradients $\Delta T_1 = 28^{\circ}C$ and $\Delta T_2 = 40^{\circ}C$ are presented in both Figs. 3 and 4.

In Fig. 3, we can see that the maximum power output and the voltage output of TEG are related directly to the value of temperature gradient applied to the TEG. Also, we can conclude that the output voltage is equal to V_{oc} /2 when the power is maximized TEG.

In addition, we can observe in Fig. 4, that the internal resistance value of the TEG can directly extract. It is interesting to work with this value when the harvesting power control is applied.

EXPERIMENTAL DATA ACQUISITION

The following Figs. 5 and 6, present the simulation and practical acquisition data of TEG (TEC-1 12706) at $\Delta T = 27^{\circ}C$ in order to allow tracing the curves *P–V* and *P–R*.

These results show the maximum power point of TEG used in this application with a temperature gradient $\Delta T = 27^{\circ}C$. The objective of these figures is to give important information about the control validation used in MPPT.[14]

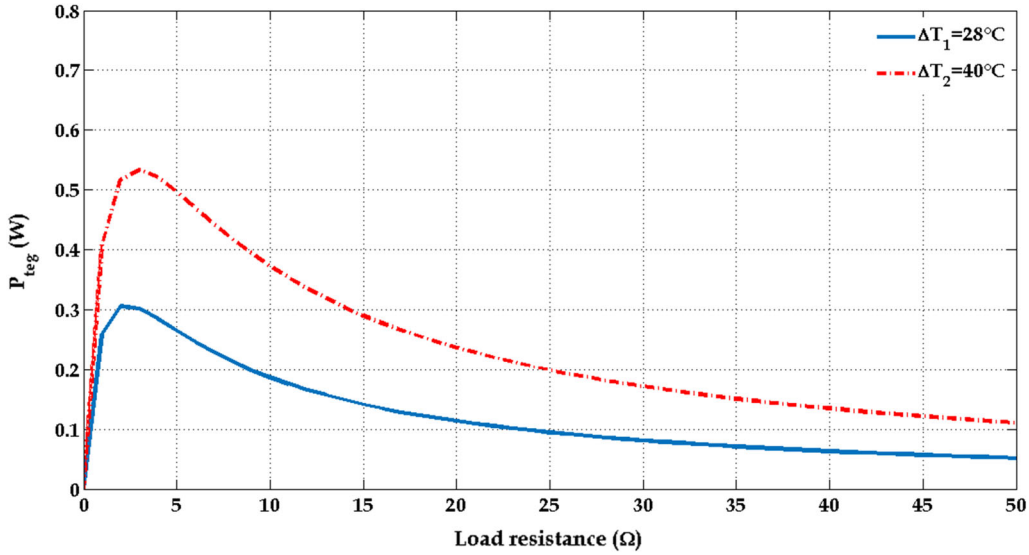

Fig. 4. *P–R* curve of TEG (TEC-1 12706). Reprinted with permission of Ref. 14.

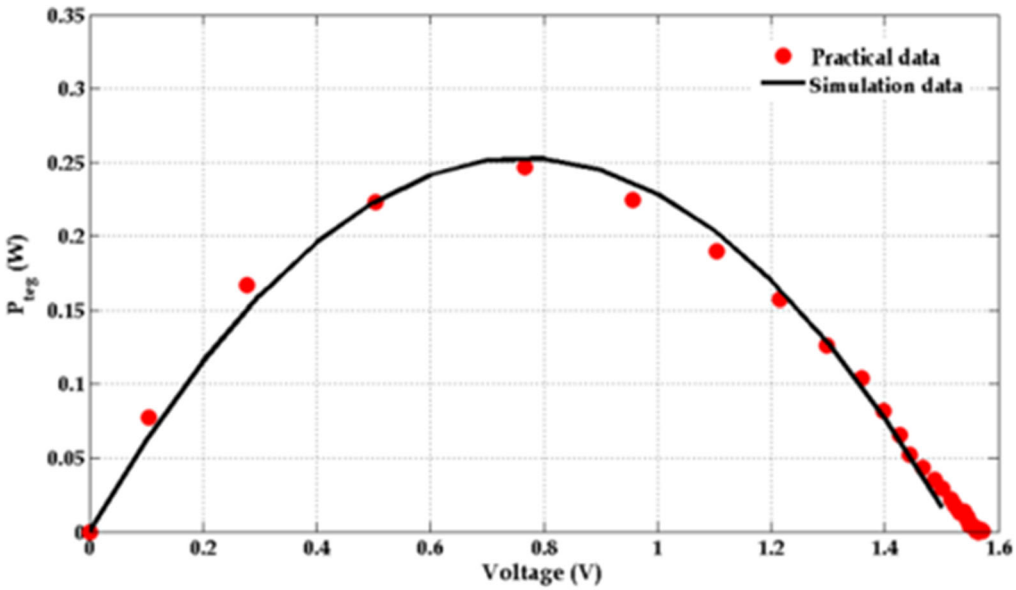

Fig. 5. Power curve of one TEG (TEC1-12706) as a function of the voltage with $\Delta T = 27°C$.

SLIDING MODE CONTROL

The sliding mode control (SMC) is well known for its robustness against internal disturbances (internal parameters system variations), external disturbances (due to the load variation), and phenomena that were omitted in the modeling phase while having a very good dynamic response.[8,26]

The purpose of this control is to characterize the surface $\sigma(x)$ on which the control objective is achieved. We recall that the sliding mode control objective consists of designing a suitable surface defined by $\sigma(x) = 0$ to restrict the state trajectories of the plan to result in the desired behavior such as tracking, regulation, and stability. Then, determine a switching control law $u(x,t)$ which is able to drive the state trajectory and maintain it on this manifold for all the time, i.e., $u(x,t)$ is determined such that the selected surface $\sigma(x)$ is made attractive and invariant.[28–31]

The sliding mode control low is divided into two parts, the first part is the equivalent control $u_{eq}(t)$ which is calculated by using the invariance condition, and the second part is the switching control $u_n(t)$ from the attractive condition.Where the sliding mode control is defined by:

$$u(t) = u_{eq}(t) + u_n(t). \quad (4)$$

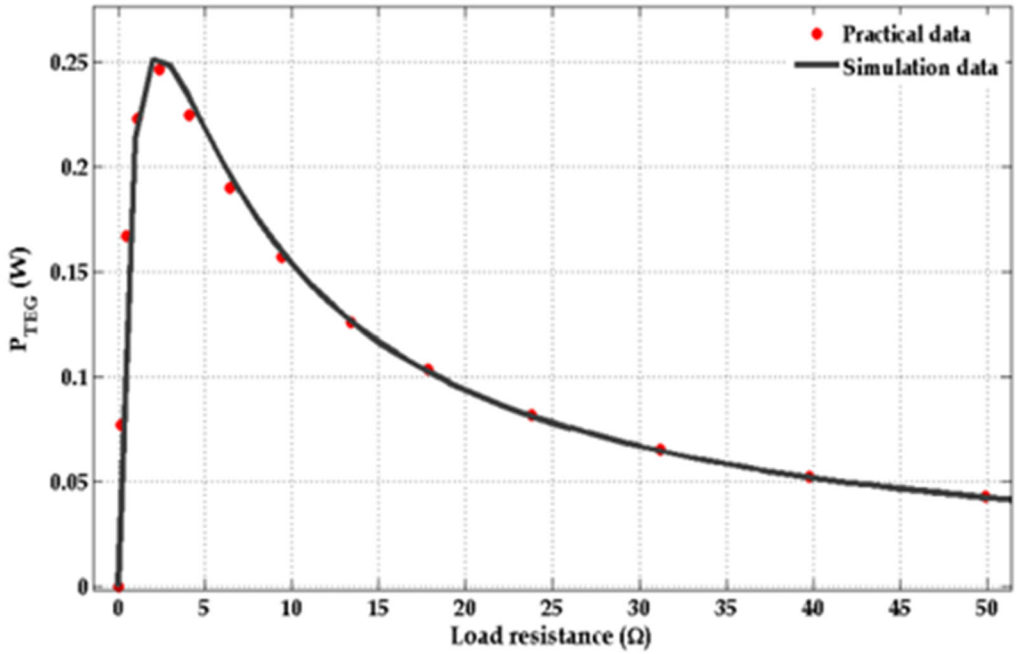

Fig. 6. Power of one TEG (TEC1-12706) as a function of the load resistance with $\Delta T = 27°C$.

To calculate these two parts of the SMC law, it must initially propose the suitable sliding surface σ.[28–31]

The main purpose is to track the maximum power point of the thermoelectric generator, which means that the power derivative equals zero $\left(\frac{dP_{TEG}}{dt} = 0\right)$.

Sliding Surface Choice

In this case the sliding surface must be dependent on the TEG power, and it is proposed by use of the following form[28–31]:

$$\sigma = f(P_{TEG}). \tag{5}$$

Equivalent Control

This control is calculated by using the invariance condition that is given by the following equations:

$$\sigma = 0 \rightarrow \frac{d\sigma}{dt} = 0 \leftrightarrow (u = u_{eq}), \tag{6}$$

where the derivative of σ is the sliding surface.

$$\sigma = \frac{dP_{TEG}}{dt} = \frac{dV_{TEG}.I}{dt} = I.\frac{dV_{TEG}}{dt} + V_{TEG}.\frac{dI}{dt} = 0 \tag{7}$$

This proposition is based on the incremental conductance (IC) method that has been used a lot in the PV systems control.

$$\sigma = I.dV_{TEG} + V_{TEG}.dI = 0 \tag{8}$$

$$\sigma = I.\frac{dV_{TEG}}{dI} + V_{TEG}.\frac{dI}{dI} = 0 \tag{9}$$

$$\sigma = V_{TEG} + I.\frac{dV_{TEG}}{dI} = 0 \tag{10}$$

$$\frac{dV_{TEG}}{dI} = -\frac{V_{TEG}}{I} \tag{11}$$

where $-\frac{dV_{TEG}}{dI}$ is called instantaneous resistance (R) and $\frac{V_{TEG}}{I}$ is called incremental resistance (r).

$$S = R(I) - r(I) \tag{12}$$

The derivative of Eq. 12 can be given by:

$$\frac{d\sigma}{dt} = \frac{dR(I)}{dt} - \frac{dr(I)}{dt}. \tag{13}$$

Multiply Eq. 13 by $\frac{dI}{dI}$.

$$\frac{d\sigma}{dt} = \left[\frac{dR(I)}{dt} - \frac{dr(I)}{dt}\right]\frac{dI}{dI} \tag{14}$$

$$\frac{d\sigma}{dt} = \left[\frac{dR(I)}{dI} - \frac{dr(I)}{dI}\right]\frac{dI}{dt} \tag{15}$$

where $\frac{dR(I)}{dI} - \frac{dr(I)}{dI} = G \neq 0$,

$$\frac{d\sigma}{dt} = G\frac{dI}{dt} = 0. \tag{16}$$

while $I = I_L$.

The final value of the time derivative of the sliding surface is obtained as:

$$\frac{d\sigma}{dt} = \frac{dI}{dt} = 0. \tag{17}$$

$\frac{dI_L}{dt}$: is the state of the boost converter

$$\frac{dI_L}{dt} = \left[-\frac{1 - u_{eq}(t)}{L} V_0 + \frac{1}{L} V_{TEG} \right] = 0 \tag{18}$$

$$-\frac{1 - u_{eq}(t)}{L} V_0 + \frac{1}{L} V_{TEG} = 0 \tag{19}$$

$$V_0 - u_{eq}(t) V_0 = V_{TEG} \tag{20}$$

$$u_{eq}(t) V_0 = V_0 - V_{TEG} \tag{21}$$

The shape of the equivalent control is given in the following equation:

$$u_{eq}(t) = \left(1 - \frac{V_{TEG}}{V_0} \right). \tag{22}$$

The switching control $u_n(t)$ in this case is given by:

$$u_n(t) = -K \operatorname{sign}(\sigma). \tag{23}$$

Finally, the sliding mode control law is given by:

$$u(t) = u_{eq}(t) + u_n(t) = \left(1 - \frac{V_{TEG}}{V_0} \right) - K \operatorname{sign}(\sigma), \tag{24}$$

where K is a positive constant.

Simulink Block Diagram of SMC and TEG

Figure 7, represents a Simulink block diagram of a 4 thermoelectric generator adapted by sliding mode control in order to perform MPPT.

Figure 7 shows the general structure of the controlling system. The Simulink block diagram is decomposed into three large parts, a 4 TEG module connected in series, the boost converter connected with the load and a block of the sliding mode control so as to ensure the maximum power transfer of the TEG modules to the load.

The SMC block needs to measure the variables I_{teg}, V_{teg} and V_{out} in order to calculate the controlling law of Eq. 24. This block is divided into three parts, the first part represent the derivative I_{teg} and V_{teg} in order to calculate the surface, the second part

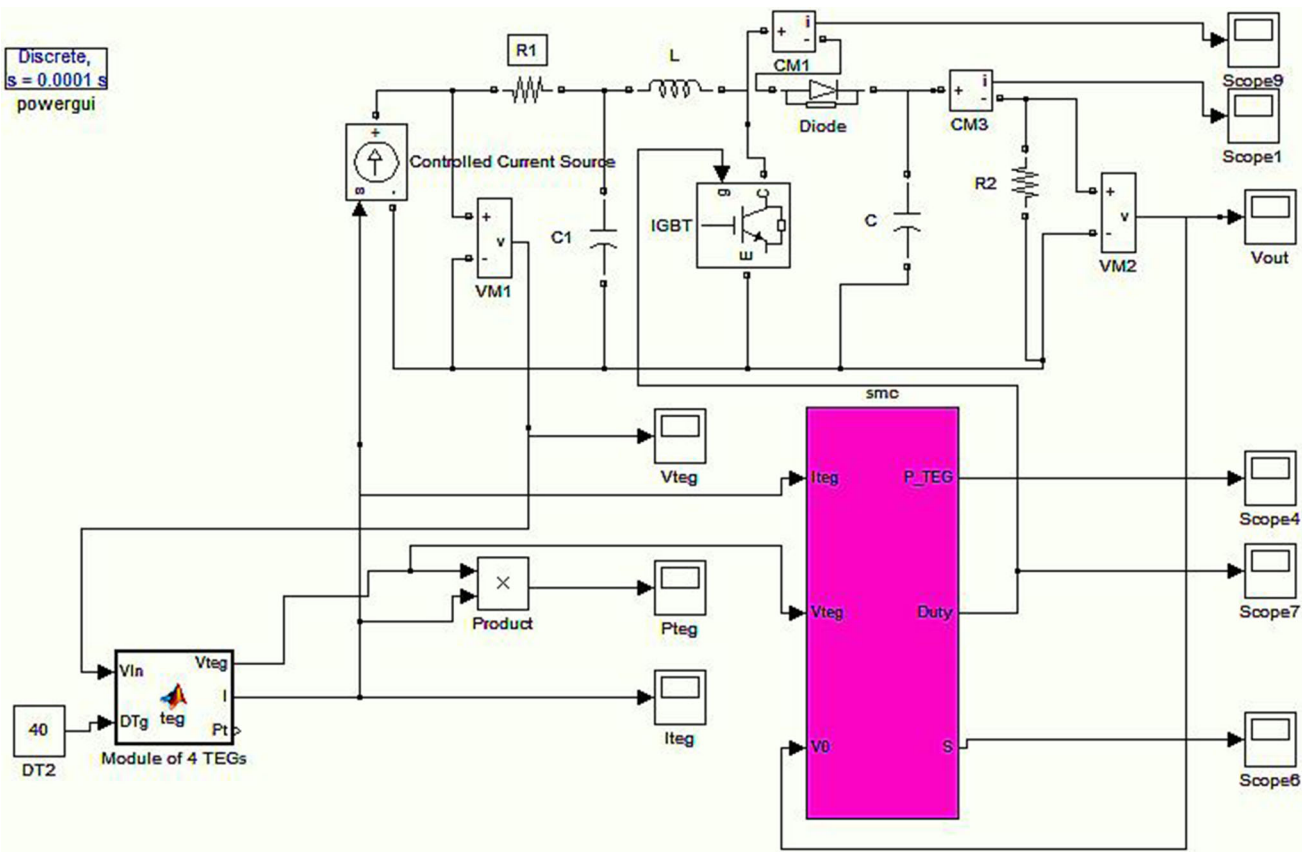

Fig. 7. Diagram of a thermoelectric generator on MATLAB/Simulink with SMC.

is to calculate the SMC law and in the third part, the controlling law converted to the PWM signal.

RESULTS AND DISCUSSION

Experimental Setup

Open source cards Arduino and the boost converter are selected for this paper in order to effectively simplify the application. These cards must be connected, firstly to the low-power amplifiers to isolate and measure the difference parameters of TEG, and secondly to the Matlab/Simulink environment. Two analog inputs are required to measure current I_{TEG}, voltage V_{TEG} of the TEG and V_0 of the boost converter. For experimental measurements, the Arduino Analog Read blocks are programmed in the Matlab/Simulink. The experimental setup system with implementation control circuit and synoptic schematic used, are shown in Figs. 8 and 9.

Results and Interpretations

In order to verify the performance of the sliding mode control realized in this work, two experimental tests of robustness are represented. The first test is the maximum power point tracking and the second one is the robustness of the control under external perturbation (varying load).

The following Figs. 10–12, show a simulation and experimental results of output variables TEG, respectively, I_{teg}, V_{teg} and P_{teg} with MPPT sliding mode control.

The gradient temperature applied to the TEG module composed of 4 thermoelectric (TEC1 12706) is $\Delta T \simeq 40^{\circ}\mathrm{C}$.

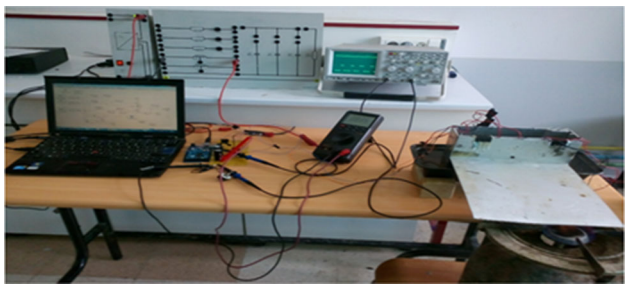

Fig. 8. Experimental setup.

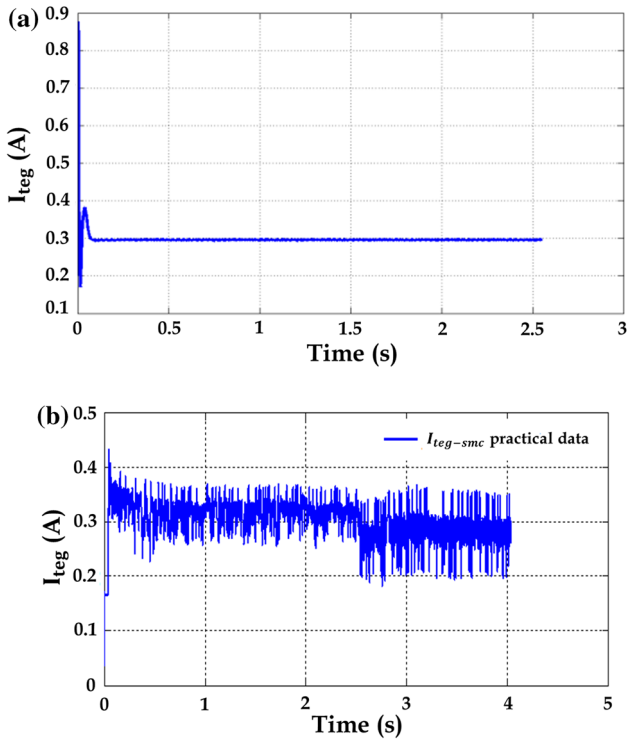

Fig. 10. Current of TEG versus the time, (a) simulation data, (b) experimental data.

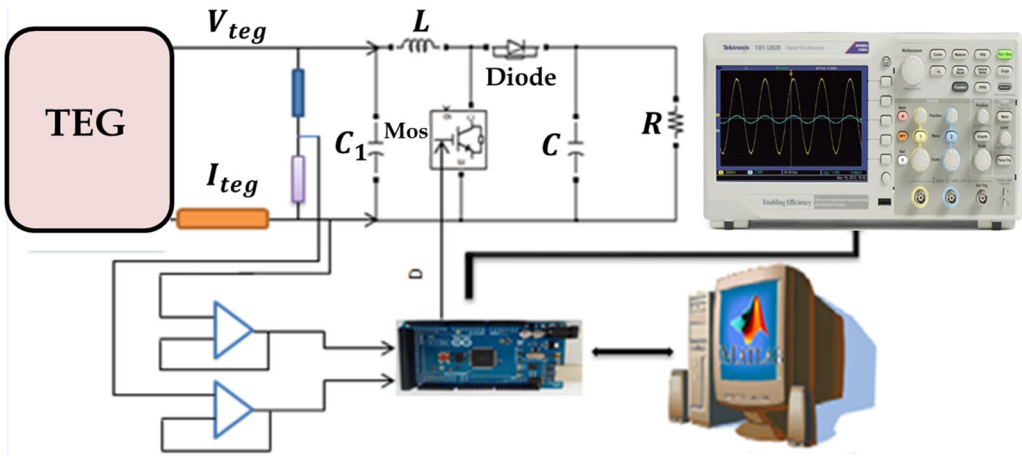

Fig. 9. Synoptic schematic of experimental setup.

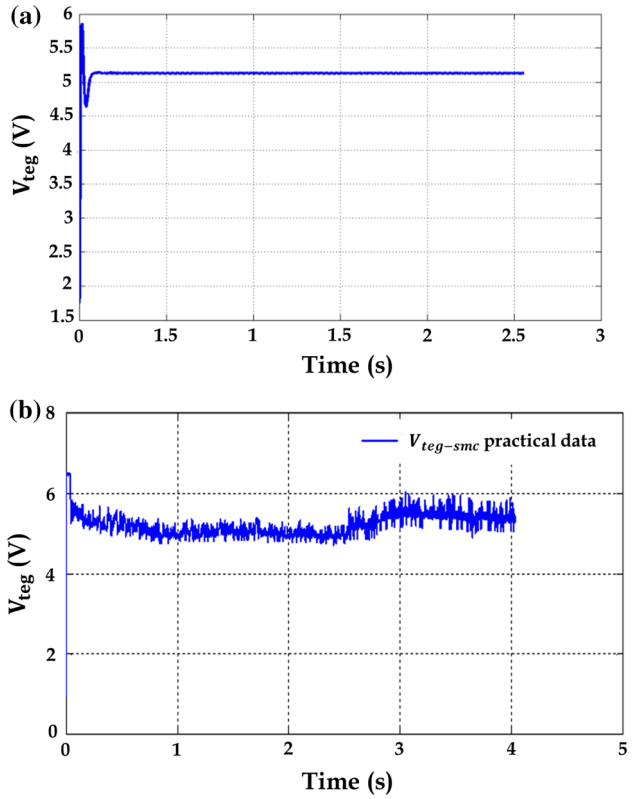

Fig. 11. Voltage of TEG versus the time, (a) simulation data, (b) experimental data.

The MPPT sliding mode control circuit measures different parameters of system (I_{TEG},V_{TEG} and V_{Load}), using the conditioners based on an operational amplifier designed to isolate the control section with the power section. The current I_{TEG} is measured by using a resistance shunt.

Figures 10b–12b, show the I_{TEG}, V_{TEG} and P_{TEG} of the TEG module when operating under a non-uniform temperature gradient. It can be seen that the output power of TEG tracks exactly its maximum, and when the external perturbation appears at t = 2.5 s, in this case, the load value is varying up to 50% (20–30 Ω). The design sliding mode control enhanced perfectly the perturbation effect. This control technique has ensured the maximum power transfer of TEG under these conditions, which mean that it achieved its main purpose.

We compared the results with the implementation of this technique by other ones found in the literature, as Paraskevas et al.,[1] Montecucco et al.[11] and Hocksun et al.,[32] from which can be noticed, that this method has a fast response, no loss of transfer power, very robust with internal disturbances (internal parameters), 0 and external disturbances (variation of the temperatures gradient and the load variation).

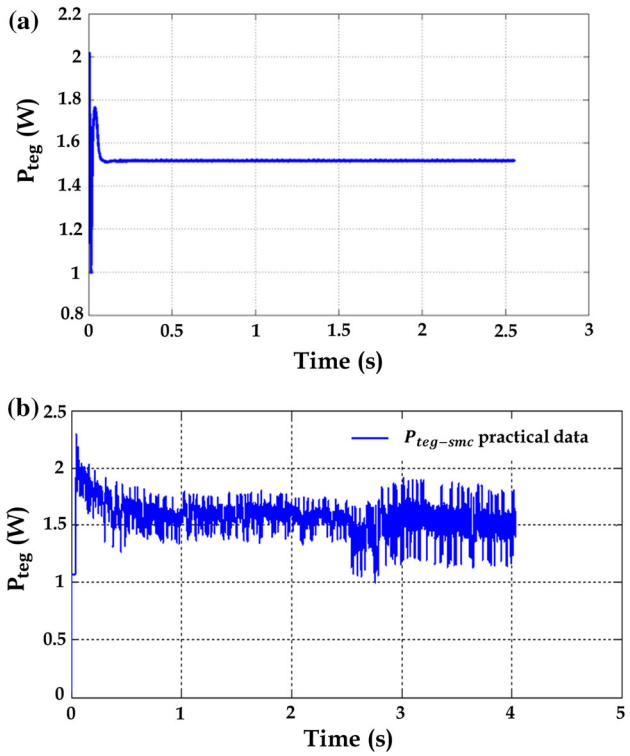

Fig. 12. The power of TEG versus the time, (a) simulation data, (b) experimental data.

CONCLUSION

In this paper, a novel method of control based on sliding mode control was proposed for TEG energy harvesting systems. These works are divided into two parts; the first of which is based on the structural mechanical development of TEG. And, the second part is focused on the development of control for maximizing transfer power. The presented system based on SMC implemented with an Arduino open source card for harvesting the Maximum Power of TEGs is studied. The proposed technique is based on an adaptation resistor controlling a power converter, which is located close to the MPP of the power-voltage curve of the TEG power source. The proposed scheme is validated analytically, experimentally, and demonstrated successful performance. The sliding mode control technique presented validates its robustness toward the high external perturbation.

REFERENCES

1. A. Paraskevas and E. Koutroulis, *Energy. Convers. Manag.* 108, 355 (2016).
2. J.P. Im, S.W. Wang, S.T. Ryu, and G.H. Cho, *IEEE J. Solid-State Circuits* 47, 3055 (2012).
3. J. Kim and C. Kim, *IEEE Trans. Power Electron.* 28, 3827 (2013).
4. N. Phillip, O. Maganga, K.J. Burnham, M.A. Ellis, S. Robinson, J. Dunn, and C. Rouaud, *J. Electron. Mater.* 42, 1900 (2013).

5. S. Dalola, M. Ferrari, V. Ferrari, M. Guizzetti, D. Marioli, and A. Taroni, *IEEE Trans. Instrum. Meas.* 58, 99 (2009).
6. P.S. Weng, H.Y. Tang, P.C. Ku, and L.H. Lu, *IEEE J. Solid-State Circuits* 48, 1031 (2013).
7. E. Brownell and M. Hodes, *IEEE Trans. Comp. Packag. Manuf. Technol.* 4, 612 (2014).
8. K. Dahech, M. Allouche, T. Damak, and F. Tadeo, *Electr. Power Syst. Res.* 143, 182 (2017).
9. D. Galayko and P. Basset, in *Proceedings of Power MEMS 2008 + microEMS*, Sendai, Japan, 2008, pp. 9–12.
10. J.D. Park, H. Lee, and M. Bond, *Energy Convers. Manag.* 86, 233 (2014).
11. A. Montecucco and A.R. Knox, *IEEE Trans. Power Electron.* 30, 828 (2015).
12. J. Eakburanawat and I. Boonyaroonate, *Appl. Energy* 83, 687 (2006).
13. C.E. Kinsella, S.M. O'Shaughnessy, M.J. Deasy, M. Duffy, and A.J. Robinson, *Appl. Energy* 114, 80 (2014).
14. S. Benahdouga, R. Khenfer, M. Meddad, A. Eddiai, and K. Benkhouja, *Mol. Cryst. Liq. Cryst.* 628, 41 (2016).
15. S.B. Riffat and X. Ma, *Appl. Therm. Eng.* 23, 913 (2003).
16. D. Dai, Y. Zhou, and J. Liu, *Renew. Energy* 36, 3530 (2011).
17. S.F. Tie and C.W. Tan, *Renew. Sustain. Energy Rev.* 20, 82 (2013).
18. K.R. Ullah, R. Saidur, H.W. Ping, R.K. Akikur, and N.H. Shuvo, *Renew. Sustain. Energy Rev.* 24, 499 (2013).
19. B.D.O. Anderson and J.B. Moore, *Linear Optimal Control* (Englewood Cliffs, NJ: Prentice-Hall, Inc., 1971).
20. Y. Yang, X.J. Wei, and J. Liu, *J. Phys. D Appl. Phys.* 40, 5790 (2007).
21. C. Wu, *Appl. Therm. Eng.* 16, 63 (1996).
22. Y.Y. Hsiao, W.C. Chang, and S.L. Chen, *Energy* 35, 1447 (2010).
23. X. Gou, H. Xiao, and S. Yang, *Appl. Energy* 87, 3131 (2010).
24. R. Yang, G. Chen, A.R. Kumar, G.J. Snyder, and J.P. Fleurial, *Energy Convers. Manag.* 46, 1407 (2005).
25. K. Yazawa and A. Shakouri, *Environ. Sci. Technol.* 45, 7548 (2011).
26. D. Nemir and J. Beck, *J. Electron. Mater.* 39, 1897 (2010).
27. L. Janak, Z. Ancik, and Z. Hadas, *Mechatronics* 2013, ed. T. Březina and R. Jablonski (Cham: Springer, 2014), pp. 265–271.
28. S. Benahdouga, D. Boukhetala, and F. Boudjema, *Electr. Power Energy Syst.* 43, 1081 (2012).
29. J. Ghazanfari and M.M. Farsangi, *Iran. J. Electric. Electron. Eng.* 9, 189 (2013).
30. A. Prabhakaran and A.S. Mathew, *Int. Res. J. Eng. Technol.* 3, 1600 (2016).
31. D. Rekioua, A.Y. Achour, and T. Rekioua, *Energy Proc.* 36, 219 (2013).
32. T.H. Kwan and X. Wu, *Energy Proc.* 105, 14 (2017).